The role of pre-therapy quantitative imaging and dosimetry in radioiodine therapy for advanced thyroid cancer

Jan Taprogge[1,2,*], Carla Abreu[1,2], Siraj Yusuf[3], Gemma Ainsworth[4], Rachel H Phillip[4], Jonathan I Gear[1,2], Rebecca Gregory[1,2], Francesca Leek[1,2], Iain Murray[1,2], Amy B Coulson[4], Sarah R Brown[4], Yong Du[3], Kate Newbold[5], Jonathan Wadsley[6], and Glenn D Flux[1,2]

1 = Joint Department of Physics, Royal Marsden NHSFT, Downs Road, Sutton, SM2 5PT, United Kingdom

2 = The Institute of Cancer Research, 123 Old Brompton Road, London, SW7 3RP, UK

3 = Department of Nuclear Medicine and PET/CT, Royal Marsden NHSFT, Downs Road, Sutton, SM2 5PT, United Kingdom

4 = Clinical Trials Research Unit, Leeds Institute of Clinical Trials Research, University of Leeds, Leeds, LS2 9JT, United Kingdom

5 = Thyroid Unit, Royal Marsden NHSFT, Downs Road, Sutton, SM2 5PT, United Kingdom

6 = Department of Oncology, Weston Park Hospital, Whitham Road, Sheffield, S10 2SJ, United Kingdom

* Corresponding/first author: Jan Taprogge, PhD, Royal Marsden NHSFT/Institute of Cancer Research, Downs Rd., Sutton, SM2 5PT, UK; +442086613033; jan.taprogge@icr.ac.uk, Reprints not available. ORCID: 0000-0001-9947-2857

Financial support for the work: Cancer Research UK (CRUK), AstraZeneca UK Limited (AZ) funded this trial (CRUK reference CRUK/14/041), NIHR Biomedical Research Centre at RMH/ICR, National Institute for Health Research (NIHR), Sanofi Genzyme (SG) provided rhTSH.

Short-title: Imaging dosimetry advance thyroid cancer

ABSTRACT

Radioactive iodine is well established as a successful treatment for differentiated thyroid cancer (DTC), although around 15% of patients have local recurrence or develop distant metastases and may become radioiodine (RAI) refractory. A personalised approach to treatment, based on the radiation absorbed doses delivered and using treatments to enhance radioiodine uptake, has not yet been developed. **Methods:** We performed a multi-centre clinical trial to investigate the role of Selumetinib which modulates the expression of the sodium iodide symporter, and hence iodine uptake, in the treatment of RAI refractory DTC. The iodine uptake pre- and post-Selumetinib was quantified to assess the effect of Selumetinib. The range of absorbed doses delivered to metastatic disease was calculated from pre- and post-therapy imaging and the predictive accuracy of a theragnostic approach to enable personalised treatment planning investigated. **Results:** Significant inter- and intra-patient variability was observed with respect to the uptake of RAI and the effect of Selumetinib. The absorbed doses delivered to metastatic lesions ranged from <1 Gy to 1170 Gy. A strong positive correlation was found between the absorbed doses predicted from pre-therapy imaging and those measured following therapy ($r=0.93$, $p < 0.001$). **Conclusion:** The variation of outcomes from RAI therapy of DTC may be explained, among other factors, by the range of absorbed doses delivered. The ability to assess the effect of treatments which modulate radioiodine uptake, and to estimate the absorbed doses at therapy introduces the potential for patient stratification using a theragnostic approach. Patient-specific absorbed dose planning could be the key to more successful treatment of advanced DTC.

Keywords: Dosimetry, Radioiodine, Theragnostics, Advanced Thyroid Cancer

INTRODUCTION

Differentiated thyroid cancer (DTC) has been treated with radioactive iodine (RAI) for over 80 years (*1*). More than 580,000 new DTC cases were estimated world-wide for 2020 (*2*). Although 84% patients survive for 10 years or more (*3*), over 15% of patients have local recurrence or develop distant metastases, and 5-10% eventually become RAI refractory (*4,5*). This carries a poor prognosis with median overall survival from three to five years. Treatment with either lithium carbonate, retinoic acid or histone deacetylases inhibitors has been attempted to re-sensitise disease to radioiodine treatment but no significant clinical benefit has been demonstrated. (*3,4*)

Initial results have shown that MAPK/ERK pathway inhibitors such as the mitogen activated protein kinase kinase (MEK) inhibitor Selumetinib (ARRY-1428860) could be used to increase sodium iodide symporter expression and restore or enhance uptake of RAI (*6-8*). Further benefit may be gained from a theragnostic approach (*9*), which offers the possibility of personalised treatments by combining therapeutics and diagnostics. In the case of RAI for DTC, the widely available imaging isotope ^{123}I-NaI may be used to guide treatment with ^{131}I-NaI and to predict the absorbed doses delivered to lesions and to healthy organs (*10,11*).

Here we report the imaging and dosimetry results from a phase 2 trial (SEL-I-METRY, EudraCT No 2015-002269-47) to re-sensitise RAI refractory DTC to further RAI therapy (*12,13*). The aims of this aspect of the trial were to establish the quantitative increase in RAI uptake due to Selumetinib and the range of absorbed doses delivered to metastatic disease from fixed levels of administered activity. In addition, we aimed to determine the accuracy with which the absorbed doses delivered

at therapy may be predicted from pre-therapy diagnostic studies and to establish the percentage of lesions responding to treatment.

MATERIALS AND METHODS

Study Design

SEL-I-METRY (EudraCT No 2015-002269-47), a phase 2 multi-centre trial, investigated the potential of Selumetinib (ARRY-1428860) to re-sensitise RAI refractory DTC to further RAI therapy (*12,13*). Patient inclusion/exclusion criteria are provided in Supplemental Table 1. Iodine refractory disease was defined as one or more lesion(s) with no measurable iodine uptake or an iodine-avid lesion that progressed within 12 months of RAI. An exploratory endpoint of the SEL-I-METRY trial was to assess the feasibility of quantitative imaging and SPECT/CT-based lesion dosimetry to personalise treatment for patients with advanced DTC.

Participants received 75 mg of Selumetinib orally twice daily for four weeks (Figure 1). Pre- and post-Selumetinib quantitative ^{123}I-NaI SPECT/CT and whole-body (WB) scans were used to predict the increase in ^{131}I-NaI uptake for subsequent treatment following the initial four weeks of Selumetinib. Patients with an increase in ^{123}I-NaI uptake of >30% following Selumetinib in at least one lesion went on to receive RAI therapy with a fixed activity of 5.5 GBq ^{131}I-NaI (*13*). Patients continued Selumetinib until the ^{131}I-NaI therapy (maximum 18 days) during the ^{123}I-NaI scan review.

For patients eligible for therapy, ^{123}I-NaI dosimetry, following the four weeks of Selumetinib administration, (hereafter referred to as pre-therapy dosimetry) and post

^{131}I-NaI therapy lesional dosimetry (hereafter referred to as post-therapy dosimetry) were performed. Pre-therapy dosimetry consisted of up to five SPECT/CT scans at 5, 24, 30, 48, and 72 hours following administration of 370 MBq ^{123}I-NaI. Following ^{131}I-NaI therapy, four post-therapy SPECT/CT scans were performed at 24, 48, 72, and 144 hours (Figure 1). Recombinant human thyroid-stimulating hormone (rhTSH) stimulation was administered before ^{123}I-NaI and ^{131}I-NaI. Imaging and reconstruction protocol are provided in Supplemental Table 2 and 3.

The study was approved by East Midlands, Leicester South Research Ethics Committee (15/EM/0455), the institutional review boards of participating centres, and the Medicines and Healthcare Products Regulatory Agency. All patients provided written informed consent prior to trial registration.

Quantitative Imaging to Assess Effect of Selumetinib

Gamma cameras at participating centres were configured for quantitative imaging including the determination of calibration factors for ^{123}I-NaI and ^{131}I-NaI, and dead-time correction factors for ^{131}I-NaI (*14*). Anatomical lesion volumes were outlined by a trained radiologist on each of the CT components of up to five post-Selumetinib ^{123}I-NaI SPECT/CT scans. Lesions were excluded from the analysis if the largest diameter was smaller than 10 mm. Oversized volumes-of-interest, encompassing all visible activity from within the lesions were delineated to determine activity retention in all ^{123}I-NaI and ^{131}I-NaI SPECT/CT images. This approach was used to minimise problems arising from breathing motion and partial volume effects and, therefore, allows for dosimetry estimates of small lesions.

The effect of Selumetinib was assessed by calculating the absolute and relative differences in ^{131}I-NaI lesion uptake during therapy predicted from the pre- and post-

Selumetinib ^{123}I-NaI images. These were converted to predictions of ^{131}I-NaI uptake during therapy taking into account the differences in physical half-lives and administered activities.

Predictive Accuracy of Pre-therapy Dosimetry and Treatment Planning

Pre-therapy dosimetry was performed to predict lesional absorbed doses during ^{131}I-NaI therapy, taking into account the differences in physical half-life and injected activities, to investigate the potential of personalised treatment planning in this patient cohort. Dosimetry was performed according to MIRD formalism (*15*) using mass-adjusted S-values and only taking into account self-dose (*16*). Uncertainties of absorbed doses were estimated according to EANM guidance (*17*).

Predictive accuracy of the pre-therapy dosimetry was assessed by calculating the absolute and relative differences between the absorbed doses predicted pre-therapy and those measured post-therapy.

Lesion Response Assessment

Response following RAI treatment was assessed using RECIST (*18*) criteria. The analysis was performed on a lesion-by-lesion basis between baseline CT scan and latest follow-up CT scan (maximum 12 months) following RAI treatment. Complete response (CR) was defined as disappearance of lesion. Partial response (PR) was established as a ≥30% decrease in lesion size (longest axis in mm). Progressive disease (PD) was defined as ≥20% increase in lesion size (longest axis in mm). Stable disease corresponded to not observing CR, PR or PD. Overall response was defined as observing either CR or PR while clinical benefit was defined as achieving CR, PR or stable disease.

Statistical Analysis

The Kruskal-Wallis test was employed to assess if relative change in quantitative uptake measurements of lesions pre- and post-Selumetinib treatment was significantly different between patients. The relationship between relative change in quantitative uptake measurements of lesions pre- and post-Selumetinib treatment and the baseline uptake in lesions was assessed using Spearman's rank correlation coefficient. The relationship between absorbed doses from pre-therapy and post-therapy dosimetry was assessed using Pearson product-moment correlation coefficients. To account for the possibility of multiple, non-independent, lesions within a single patient, all correlation coefficients were calculated on group-mean centred data.

The relationships between post-Selumetinib uptake and absorbed doses, respectively, and baseline data, biomarkers, and Selumetinib treatment parameters were explored. A multi-level modelling approach was employed to account for the nested data structure, incorporating random effects with respect to each patient. Lesional variables (baseline CT lesion size) were explored as fixed effects within the model. Patient level variables (cancer subtype, sum of CT lesion size, thyroglobulin, and total Selumetinib dose) were explored as random effects in the model. All models were adjusted for pre-Selumetinib lesion uptake or pre-therapy predicted absorbed doses, respectively, as a fixed effect. A forward selection approach with Chi-squared testing was used to decide which variables to include in the model. Chi-squared tests were used to test the difference between the nested models and determine whether inclusion of a variable improved model fit.

The association between quantitative absorbed doses from pre- and post-Selumetinib therapy ^{123}I-NaI and ^{131}I-NaI imaging with treatment success was investigated using univariate logistic regression modelling. Additionally, receiver operating curve analysis of the data was explored to establish a threshold absorbed dose for overall response rate and clinical benefit rate, using cut-offs at the median, 1/3 and 2/3 quantiles.

All statistical tests were exploratory as the trial was not formally powered to detect statistically significant effects on the dosimetry endpoints. Testing was performed at the two-sided 5% significance level and did not account for multiple testing. Statistical analysis was performed using R version 4.0.2 or later versions and the Kruskal-Wallis test was performed using GraphPad Prism version 9.3.1 for Windows (GraphPad Software, San Diego, California USA, www.graphpad.com).

RESULTS

Thirty RAI refractory DTC patients were recruited to SEL-I-METRY, a phase 2 multi-centre trial, of whom 28 received Selumetinib treatment. Nine patients (patient characteristics in Table 1) demonstrated an increase in ^{123}I-NaI uptake after 4 weeks of Selumetinib (demonstrated in Figure 2) of 30% or more and were administered RAI treatment after a median of 12.5 (range 2 to 15) days. During this time, the patients continued to take Selumetinib. Within these nine patients, a total of 39 lesions were identified. Median lesion volume was 2.6 ml (minimum: 0.3 ml, 25th percentile: 0.7 ml, 75th percentile: 9.6 ml, maximum: 43.1 ml). Eighteen lesions were located in the lungs, fourteen in bone, and seven in soft tissues (four in lymph nodes and three in the thyroid bed/neck area).

Quantitative Imaging to Assess Effect of Selumetinib

Quantitative single-photon emission computerized tomography *(*SPECT*)* imaging before and after treatment with Selumetinib was used to assess the effect of Selumetinib on RAI uptake. Two lesions were excluded from this analysis as they were not included in the range of the pre-Selumetinib scan. Median predicted ^{131}I-NaI uptake per lesion volume (MBq/cc) at 24 hours in 37 lesions pre- and post-Selumetinib were 0.2 MBq/cc (range 0.001 to 11.5 MBq/cc) and 2.1 MBq (range 0.01 to 175.4 MBq/cc), respectively. Median absolute (predicted uptake post-Selumetinib minus predicted uptake pre-Selumetinib) and relative (predicted uptake post-Selumetinib divided by uptake pre-Selumetinib) change was 1.9 MBq/cc (range -0.4 to 174.9 MBq/cc) and 16.7 (range 0.7 to 819.1), respectively. Figure 3 shows the relative change in predicted ^{131}I-NaI uptake. The absolute and relative change in uptake are presented in Figures 4 and 5, respectively, with respect to the baseline uptake.

A large inter- and intra-patient variability was observed for the relative change in uptake on a lesional basis. A Kruskal-Wallis test showed that relative increase in uptake was significantly different between patients ($H(8) = 22.48$, $p=0.004$). There was a weak, positive correlation between the group-mean centred data of the relative uptake change and the baseline uptake pre-Selumetinib (see Supplemental Figure 1), $r(37) = .011$; however, the relationship was not significant ($p = .946$).

A multi-level modelling approach was used to assess the relationships between post-Selumetinib uptake, adjusted for pre-Selumetinib lesion uptake, and baseline data, biomarkers, and Selumetinib treatment parameters. No variables of interest improved the multi-level model fit over and above the null model according to the chi-squared difference tests, with many models demonstrating singular fit, likely caused

by the small sample size being unable to support the complexity of the modelling approach. The intraclass correlation coefficient was calculated as 0.093 for patients, indicating large variability.

Predictive Accuracy of Pre-therapy Dosimetry

To assess the feasibility of applying theragnostic and dosimetry-based treatment planning in this patient cohort, pre- and post-therapy dosimetry was performed to assess the absorbed doses delivered to the lesions and to investigate whether pre-therapy imaging can be used for treatment planning. All 39 lesions were evaluated for dosimetry. Median predicted absorbed doses from pre-therapy and post-therapy dosimetry were 17.2 Gy (range 0.1 to 1292.1 Gy) and 10.4 Gy (range 0.3 to 1169.9 Gy), respectively. The median relative percentage difference between pre-therapy and post-therapy dosimetry was found to be -33% (range -98 to 764%).

Comparison of predicted absorbed doses prior to therapy and measured absorbed doses following RAI therapy are shown in Figure 6, illustrating the wide range of absorbed doses delivered. Pearson product-moment correlation analysis of the group-mean centred data (Supplemental Figure 2) resulted in a strong positive correlation between the predicted absorbed doses from pre-therapy dosimetry and post-therapy dosimetry, $r(37)=0.93$, $p < 0.001$. Figure 7 shows a Bland-Altman plot of the difference between predicted and measured absorbed doses. The estimated bias was 37.0 Gy (SD 71.9 Gy), illustrating that predicted absorbed doses were higher than delivered absorbed doses. Supplemental Figures 3 and 4 show Bland-Altman plots of the 24 hour uptake and the retention half-lives, respectively, comparing the predicted values using pre-therapy dosimetry and those measured post-therapy.

A multi-level modelling approach was used to assess the relationships between post-therapy absorbed doses, adjusted for pre-therapy predicted absorbed doses, and baseline data, biomarkers, and Selumetinib treatment parameters. No variables of interest improved the multi-level model fit over and above the null model according to the chi-squared difference tests, again with many models demonstrating singular fit. The intraclass correlation coefficient was calculated as 0.062 for patients.

Lesion Response Analysis

Follow-up CT scans were collected for seven patients (last follow-up at: three (n=1), six (n=1), nine (n=1), and twelve (n=4) months), with a total of 24 lesions included in analysis. Response was assessed using RECIST(18) criteria but on an individual lesion basis by comparing baseline CT scan and latest follow-up scan for each patient. Overall response was defined as either complete response CR (disappearance of the lesion) or partial response PR (≥30% decrease in lesion size defined by longest axis in mm). Clinical benefit was taken to be CR, PR or stable disease (<30% decrease or increase in lesion size). Overall response and clinical benefit were observed in 13% (3/24) and 83% (20/24) of lesions, respectively.

Univariate logistic regression modelling was employed to assess the association between quantitative absorbed doses from pre- and post-Selumetinib therapy imaging and treatment success. The logistic models demonstrated poor fit due to small sample size and were highly influenced by outliers in the data, and are therefore not presented. Receiver operating curve analysis of the data was explored although was also limited by the small sample size and a threshold absorbed dose could not established.

DISCUSSION

Quantitative ^{123}I-NaI imaging has shown great potential to assess whether further ^{131}I-NaI treatment is warranted following attempted re-sensitisation of RAI refractory DTC with Selumetinib. A significant inter- and intra-patient variability was found with respect to the relative change in RAI uptake following treatment with Selumetinib in the present patient cohort. This suggests that patient-specific assessment of uptake changes before proceeding with RAI therapy should be indicated to fulfil the justification principle. Furthermore, RAI concentration within lesions before and after treatment with Selumetinib demonstrated large differences between patients but also with respect to lesions within individual patients. No patient- or lesion-specific biomarkers were identified to be predictive of uptake. Results of studies by Ho et al suggest that a biomarker-directed strategy may be required as redifferentiation using Selumetinib in BRAF^{V600E}-mutant patient appeared to be less successful (*7,19*).

The relative change in uptake was not found to be correlated with the baseline uptake suggesting Selumetinib might be effective as well in non-refractory patients, who still have a degree of iodine uptake in lesions before starting treatment. Ho et al (*19*) used Selumetinib plus RAI therapy in a phase 3 randomised clinical trial in the adjuvant treatment of high-risk, resected DTC patients but could not show a statistically significant difference in complete remission when compared to RAI therapy alone. Further investigations are warranted in the use of Selumetinib or other related drugs to improve outcome in cohorts of advanced DTC patients at risk of becoming RAI refractory.

The large range of RAI uptakes observed in patients is also reflected in the wide ranges of absorbed doses delivered to lesions from a fixed 5.5 GBq administration to patients with advanced DTC. This is considered standard practice in the UK and in line with national guidelines and was therefore used in the current study (*20*). The large range agrees with results presented previously (*21,22*) and could potentially explain the variations in outcome observed between patients. Personalised treatment planning based on the absorbed doses delivered could, therefore, potentially be warranted in in this patient cohort.

The results suggest that personalised treatment planning using pre-therapy ^{123}I-NaI is feasible. While the absolute accuracy decreases for absorbed doses higher than 50 Gy, pre-therapy dosimetry was fairly correlated with post-treatment dosimetry. The average difference of -33% may be due to differences in imaging schedules, the possibility of a stunning effect of ^{123}I-NaI or self-stunning of ^{131}I-NaI (*23,24,25*), a delayed action of the Selumetinib during the time prior to therapy, alterations of bio-kinetics due to prior administration of rhTSH (*26*), saturation of receptors or the continued use of Selumetinib prior to RAI therapy. The latter has not yet been studied. To our knowledge, this is the first time that ^{123}I-NaI pre-therapy dosimetry has been shown to be indicative of the absorbed doses delivered from treatment in metastatic DTC patients. This result could potentially have wide implications for molecular radiotherapy as it will allow for personalised treatment planning in combination with dosimetric methods to assess absorbed doses to organs-at-risk, such as whole-body and bone-marrow dosimetry (*27*).

The large uncertainties for the absorbed doses, obtained using oversized volumes-of-interest, reflect the volume estimate uncertainties for small lesions and the significantly shorter half-life of ^{123}I-NaI (*28*). Uncertainties are potentially smaller with

^{124}I-NaI pre-therapy dosimetry which was not available for this study. The longer physical half-life of ^{124}I-NaI compared to ^{123}I-NaI would allow for more accurate determination of the retention half-lives. ^{123}I-NaI pre-therapy dosimetry potentially overestimates the retention half-life (Supplemental Figure 3) and, therefore, the absorbed dose delivered.

Limitations of the present analysis include that the trial was not designed to have sufficient power to detect statistically significant effects on the dosimetry endpoints and statistical testing did not account for multiple testing. The relatively small number of patients undergoing both pre- and post-therapy dosimetry is a limiting factor, and the statistical analysis should be considered exploratory in nature. Where feasible, future studies should be sufficiently powered to detect statistically significant effects and to identify key parameters affecting both the response to treatments prior to RAI therapy and the absorbed doses delivered. Additionally, since this type of data has a nested structure of lesions within patients, careful consideration should be given to the design of trials aiming to capture this data. This will aid in avoiding or mitigating potential issues that may arise when using a multi-level modelling approach, such as the issues with model singularity encountered here. Follow-up analysis was limited due to the short follow-up time leading to inconclusive results with respect to the absorbed dose relationship due to poor model fit. Response measurements of bone lesions using RECIST criteria are considered difficult but can be performed for osteolytic lesions, the predominant type in thyroid cancer. Nevertheless, the lack of an absorbed dose relationship potentially reflects that 14 of the 39 lesions were found in bone. Similarly, an absorbed dose threshold could not be identified. The majority of absorbed doses delivered were estimated to be lower than proposed absorbed dose

thresholds for soft tissue (*29*) and bone metastases (*30*) which is in line with the low overall response rate observed of 13%.

Absorbed dose response relationships for advanced DTC (*30*) should be confirmed in multi-centre clinical trials. Together with the results presented here, this would facilitate personalised treatment planning of RAI administrations.

CONCLUSION

Quantitative SPECT/CT imaging has shown a large inter- and intra-patient variability in the effect of Selumetinib in increasing the RAI uptake in lesions in advanced RAI refractory DTC. In addition, a large range of RAI uptake concentration in lesions at baseline is observed. The absorbed doses delivered at therapy in this patient cohort can be estimated from a pre-therapy dosimetry study.

These findings suggest that future studies of redifferentiation therapy should utilise the combination of pre-therapy quantitative imaging, to assess the effect of treatments to enhance RAI uptake, and dosimetry, to plan the activity of RAI administered to patients, to ensure that those patients achieving increased iodine uptake obtain maximum benefit from subsequent therapy.

Our findings also likely have implications for the personalised treatment planning of patients with iodine sensitive DTC.

DISCLOSURE

SRB, GF, JW, JT, IM, JG, CA report funding and/or provision of study materials from CRUK, Astrazeneca and Sanofi Genzyme during the conduct of the study. JT, CA, JG, IM and GF report funding from National Health Service to the NIHR Biomedical Research Centre at The Royal Marsden and the ICR and grants from Euratom research and training programme 2014-2018 and National Institute for Health Research (NIHR) and NIHR Royal Marsden Clinical Research Facility. JG reports personal fees and honoraria from The European Association of Nuclear Medicine. JW reports personal fees and honoraria from Lilly, Eisai, Novartis, AAA, Bayer, Ipsen and Roche. ABC reports grants and non-financial support from BMS/Celgene, Merck Sharpe & Dohme, Amgen and Takeda. No other potential conflicts of interest relevant to this article exist.

ACKNOWLEDGMENTS

The authors are deeply indebted to the participants and their families and carers. Cancer Research UK (CRUK, reference CRUK/14/041) and AstraZeneca UK Limited funded this trial. Sanofi Genzyme provided rhTSH. The research was developed with support from NCRI CTRad. NHS funding was provided to the NIHR Biomedical Research Centre at The Royal Marsden and the ICR. The RTTQA group is funded by the National Institute for Health and Care Research (NIHR). We acknowledge infrastructure support from the NIHR Royal Marsden Clinical Research Facility Funding. This report is independent research funded by the NIHR. The views expressed in this publication are those of the author(s) and not necessarily those of the NHS, the NIHR or the Department of Health and Social Care.

The authors are grateful to the SEL-I-METRY teams at the participating hospitals and the Trial Steering Committee and Data Monitoring and Ethics Committee members, for whom the trial would not have been possible without.

CONTRIBUTIONS

JT, CA, JG, RG, FL, IM, YD, KN, SRB, JW and GF designed and performed the study. JT, CA, SY, JG, RG, FL, IM and GF analysed the data. JT, GA, RHP, ABC and SRB performed statistical analysis. JT, GA, JG, IM, ABC, SRB, KN, JW and GF wrote the manuscript. All authors reviewed and approved the final manuscript.

KEY POINTS

Question: Can quantitative imaging and SPECT/CT-based lesional dosimetry be used to personalise radioiodine treatment for advanced thyroid cancer which currently has a poor prognosis?

Pertinent findings: Quantitative imaging and dosimetry of patients with radioiodine-refractory thyroid cancer was performed as part of the phase 2 SEL-I-METRY trial (EudraCT No 2015-002269-47) which aimed to assess the possibility of re-sensitising patients to further RAI therapy. Pre-therapy imaging has proven to be a powerful tool to assist with the stratification of patients prior to further radioiodine therapy and a strong positive correlation was found between pre- and post-therapy absorbed doses, indicating the suitability of pre-therapy dosimetry for treatment planning.

Implications for patient care: Pre-therapy quantitative imaging and dosimetry in radioiodine therapy for advanced thyroid cancer has the potential to inform treatment planning for individual patients and to alter patient management.

REFERENCES

1. Hertz S, Roberts A. Radioactive iodine in the study of thyroid physiology: VII. The use of radioactive iodine therapy in hyperthyroidism. *J Am Med Assoc*. 1946;131:81-86.

2. Pizzato M, Li M, Vignat J, et al. The epidemiological landscape of thyroid cancer worldwide: GLOBOCAN estimates for incidence and mortality rates in 2020. *Lancet Diabetes Endocrinol*. 2022;10:264-272.

3. Schlumberger M, Brose M, Elisei R, et al. Definition and management of radioactive iodine-refractory differentiated thyroid cancer. *Lancet Diabetes Endocrinol*. 2014;2:356-358.

4. Jin Y, Van Nostrand D, Cheng L, Liu M, Chen L. Radioiodine refractory differentiated thyroid cancer. *Crit Rev Oncol Hematol*. 2018;125:111-120.

5. Durante C, Haddy N, Baudin E, et al. Long-term outcome of 444 patients with distant metastases from papillary and follicular thyroid carcinoma: Benefits and limits of radioiodine therapy. *J Clin Endocrinol Metab*. 2006;91:2892-2899.

6. Chakravarty D, Santos E, Ryder M, et al. Small-molecule MAPK inhibitors restore radioiodine incorporation in mouse thyroid cancers with conditional BRAF activation. *J Clin Invest*. 2011;121:4700-4711.

7. Ho AL, Grewal RK, Leboeuf R, et al. Selumetinib-enhanced radioiodine uptake in advanced thyroid cancer. *N Engl J Med*. 2013;368:623-632.

8. Rothenberg SM, McFadden DG, Palmer EL, Daniels GH, Wirth LJ. Redifferentiation of iodine-refractory BRAF V600E-mutant metastatic papillary thyroid cancer with dabrafenib. *Clin Cancer Res*. 2015;21:1028-1035.

9. Arnold C. Theranostics could be big business in precision oncology. *Nat Med*. 2022;28:606-608.

10. Van Nostrand D, Aiken M, Atkins F, et al. The utility of radioiodine scans prior to iodine-131 ablation in patients with well-differentiated thyroid cancer. *Thyroid*. 2009;19:849-855.

11. Brans B, Bodei L, Giammarile F, et al. Clinical radionuclide therapy dosimetry: the quest for the “Holy Gray”. *Eur J Nucl Med Mol Imaging*. 2007;34:772-786.

12. Wadsley J, Gregory R, Flux G, et al. SELIMETRY-a multicentre I-131 dosimetry trial: a clinical perspective. *Br J Radiol*. 2017;90:20160637-20160637.

13. Brown SR, Hall A, Buckley HL, et al. Investigating the potential clinical benefit of Selumetinib in resensitising advanced iodine refractory differentiated thyroid cancer to radioiodine therapy (SEL-I-METRY): protocol for a multicentre UK single arm phase II trial. *BMC cancer*. 2019;19:582.

14. Gregory RA, Murray I, Gear J, et al. Standardised quantitative radioiodine SPECT/CT imaging for multicentre dosimetry trials in molecular radiotherapy. *Phys Med Biol*. 2019;64:245013.

15. Bolch WE, Eckerman KF, Sgouros G, Thomas SR. MIRD pamphlet No.21: a generalized schema for radiopharmaceutical dosimetry--standardization of nomenclature. *J Nucl Med*. 2009;50:477-484.

16. Stabin MG, Siegel JA. Physical models and dose factors for use in internal dose assessment. *Health Phys*. 2003;85:294-310.

17. Gear JI, Cox MG, Gustafsson J, et al. EANM practical guidance on uncertainty analysis for molecular radiotherapy absorbed dose calculations. *Eur J Nucl Med Mol Imaging*. 2018;45:2456-2474.

18. Eisenhauer EA, Therasse P, Bogaerts J, et al. New response evaluation criteria in solid tumours: revised RECIST guideline (version1.1). *Eur J Cancer*. 2009;45:228-247.

19. Ho AL, Dedecjus M, Wirth LJ, et al. Selumetinib plus adjuvant radioactive iodine in patients with high-risk differentiated thyroid cancer: A phase III, randomized, placebo-controlled trial (ASTRA). *J Clin Oncol*. 2022;40:1870-1878.

20. Wadsley J, Armstrong N, Bassett-Smith V, et al. Patient Preparation and Radiation Protection Guidance for Adult Patients Undergoing Radioiodine Treatment for Thyroid Cancer in the UK. *Clin Oncol (R Coll Radiol)*. 2023;35:42-56.

21. de Keizer B, Brans B, Hoekstra A, et al. Tumour dosimetry and response in patients with metastatic differentiated thyroid cancer using recombinant human thyrotropin before radioiodine therapy. *Eur J Nucl Med Mol Imaging*. 2003;30:367-373.

22. Sun F, Gerrard GE, Roberts JK, et al. Ten year experience of radioiodine dosimetry: is it useful in the management of metastatic differentiated thyroid cancer? *Clin Oncol (R Coll Radiol)*. 2017;29:310-315.

23. Lassmann M, Luster M, Hänscheid H, Reiners C. Impact of 131I diagnostic activities on the biokinetics of thyroid remnants. *J Nucl Med*. 2004;45:619-625.

24. McDougall IR, Iagaru A. Thyroid stunning: fact or fiction? *Semin Nucl Med*. 2011;41:105-112.

25. Canzi C, Zito F, Voltini F, Reschini E, Gerundini P. Verification of the agreement of two dosimetric methods with radioiodine therapy in hyperthyroid patients. *Med Phys*. 2006;33:2860-2867.

26. Hänscheid H, Lassmann M, Luster M, et al. Iodine biokinetics and dosimetry in radioiodine therapy of thyroid cancer: procedures and results of a prospective international controlled study of ablation after rhTSH or hormone withdrawal. *J Nucl Med*. 2006;47:648-654.

27. Lassmann M, Hänscheid H, Chiesa C, et al. EANM Dosimetry Committee series on standard operational procedures for pre-therapeutic dosimetry I: Blood and bone marrow dosimetry in differentiated thyroid cancer therapy. *Eur J Nucl Med Mol Imaging*. 2008;35:1405-1412.

28. Flux G, Guy MJ, Beddows R, Pryor M, Flower MA. Estimation and implications of random errors in whole-body dosimetry for targeted radionuclide therapy. *Phys Med Biol*. 2002;47:3211-3223.

29. Maxon HR, Thomas SR, Hertzberg VS, et al. Relation between effective radiation dose and outcome of radioiodine therapy for thyroid cancer. *N Engl J Med. 1983*;309:937-941.

30. Jentzen E, Verschure F, van Zon A, et al. 124I-PET assessment of response of bone metastases to initial radioiodine treatment of differentiated thyroid cancer. *J Nucl Med*. 2016;57:1499-1504.

TABLES

TABLE 1: Patient characteristics.

Characteristic	Value
Median age (yr) (range)	48 (45 – 78)
Female N (%)	3 (33%)
Histology subtype – N (%)	
Papillary	2 (22%)
Follicular	7 (78%)
Median cumulated activity of RAI prior to study registration (GBq) (range)	7.6 (3.7 – 14.6)
Median baseline thyroglobulin (ug/L) (range)	742 (36 – 7530)

FIGURE LEGENDS

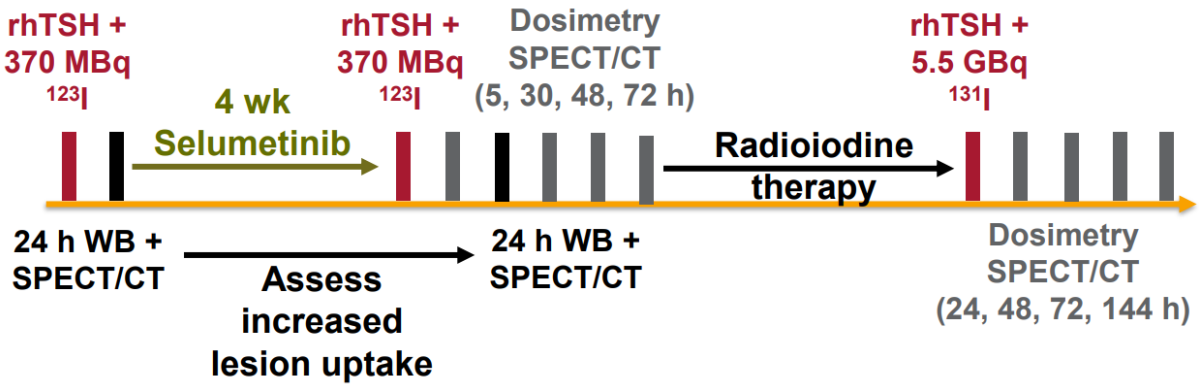

FIGURE 1: SEL-I-METRY imaging schedule consisting of 24h WB and SPECT ^{123}I-NaI scans pre-Selumetinib, a 24h WB and SPECT ^{123}I-NaI scan post-Selumetinib, up to four additional dosimetry SPECT/CT ^{123}I-NaI scans post-Selumetinib and up to four dosimetry SPECT/CT scans following treatment with 5.5 GBq of ^{131}I-NaI.

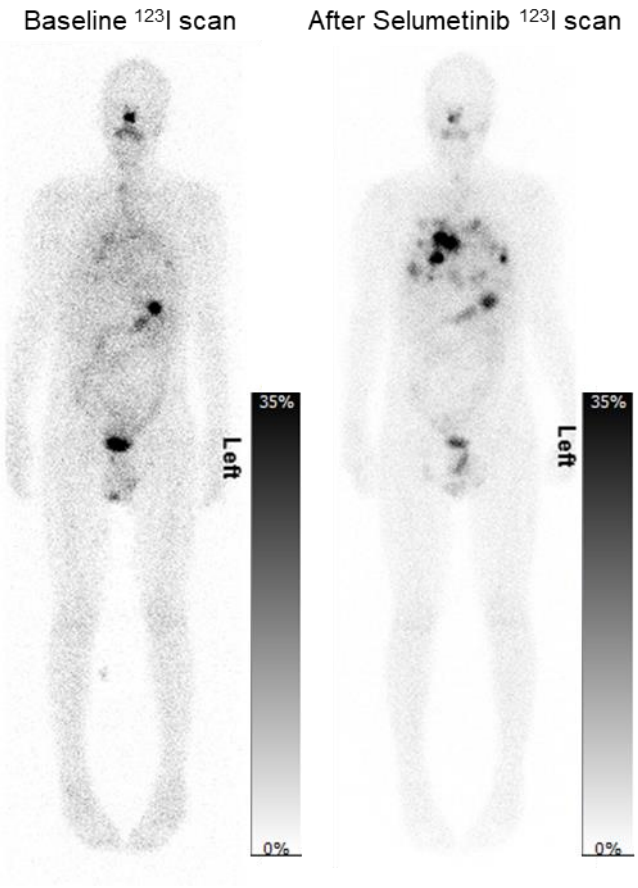

FIGURE 2: Example of whole-body planar scans at 24 hours post ^{123}I-NaI administration at a) the baseline, before Selumetinib was administered, and b) after 4 weeks of treatment with Selumetinib.

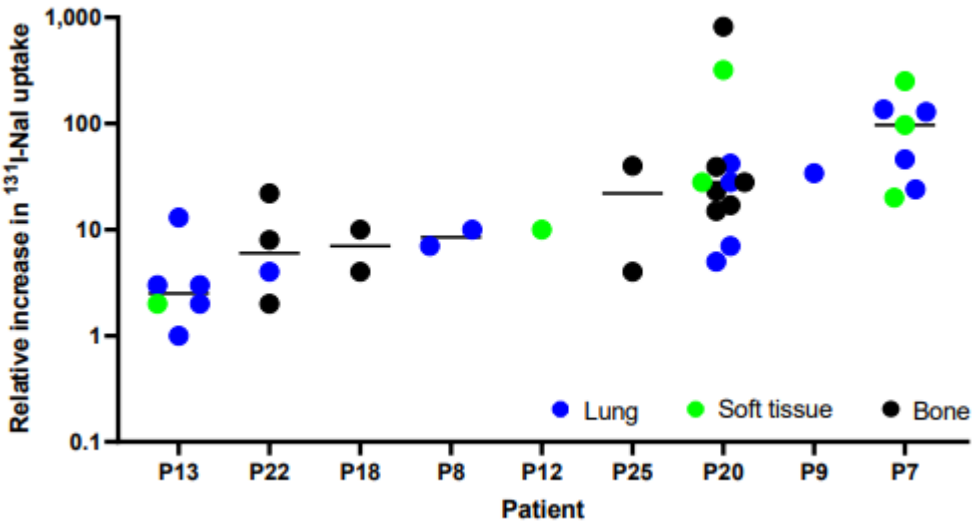

FIGURE 3: Relative change in predicted ^{131}I-NaI uptake following treatment with Selumetinib with respect to the uptake before Selumetinib administration. Relative increase in uptake is shown for the 9 patients who progressed to RAI therapy. Lesions are colour-coded based on their location (lung tissue, soft tissue and bone).

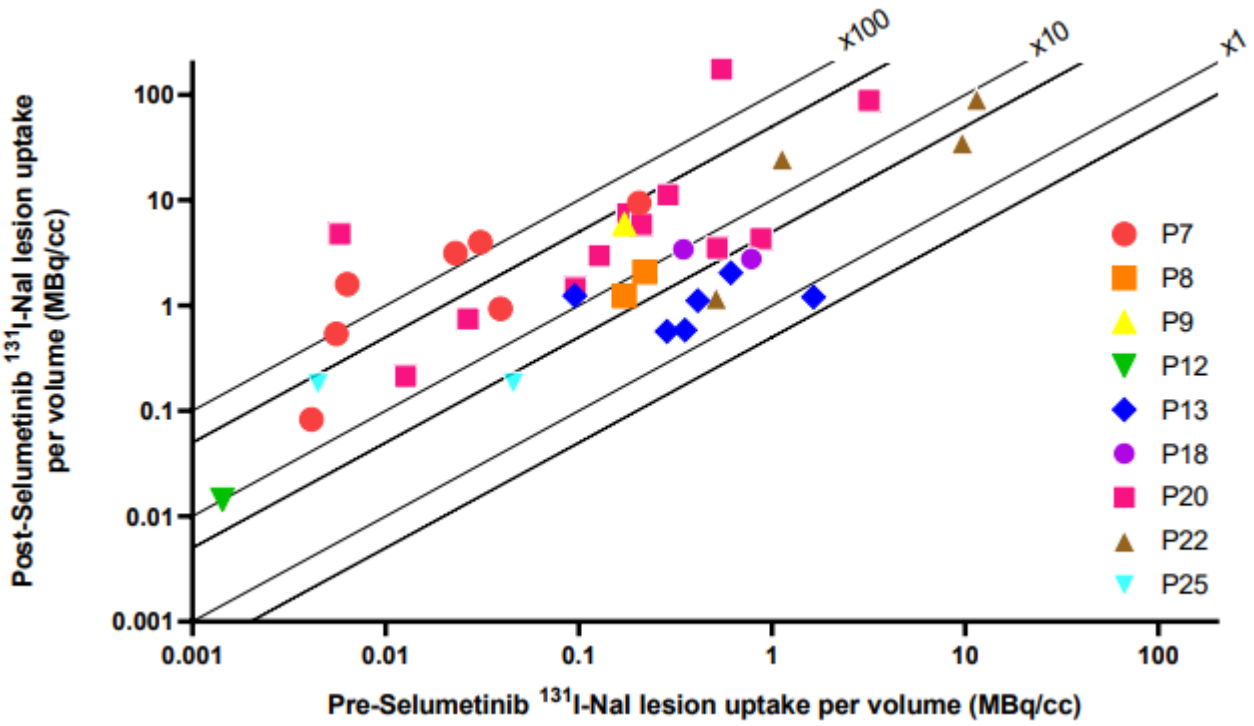

FIGURE 4: Uptake of ^{131}I-NaI before and after treatment with Selumetinib. Lesions are color-coded for individual patients. Solid lines represent a relative increase in uptake by a factor of 1, 10 and 100 respectively to illustrate the relative effect of the Selumetinib in individual patients and lesions.

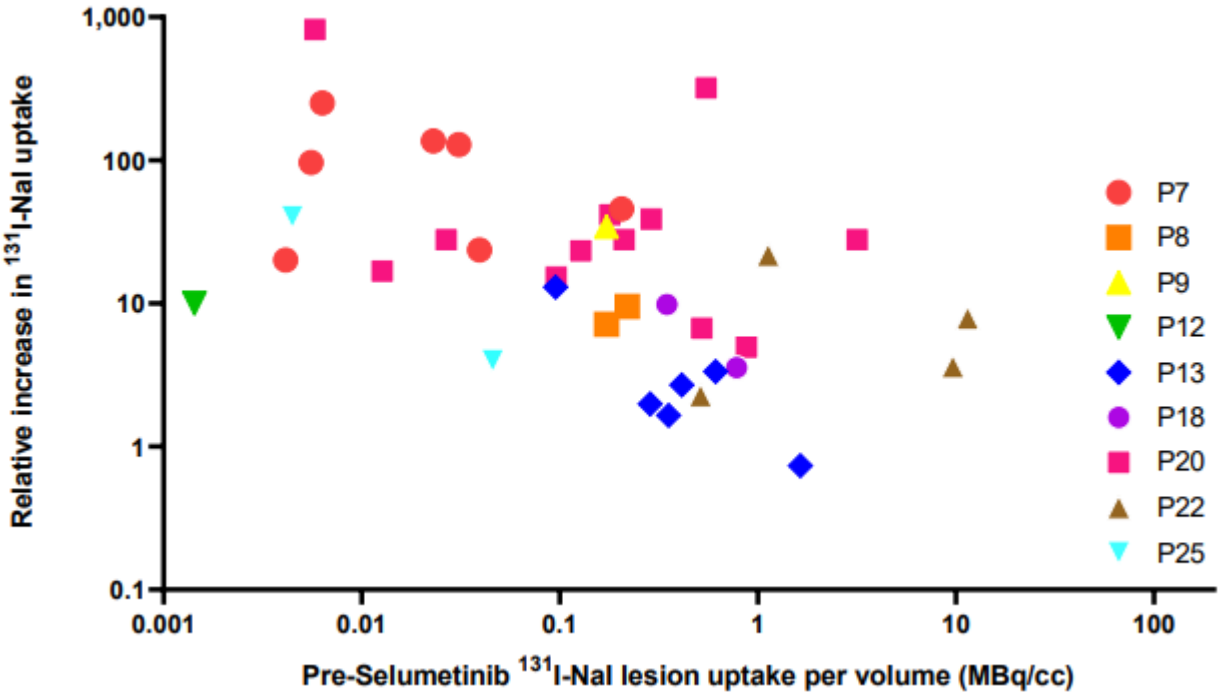

FIGURE 5: Relative increase in ^{131}I-NaI uptake following treatment with Selumetinib plotted against the baseline uptake of ^{131}I-NaI prior to treatment (colour coded by patient).

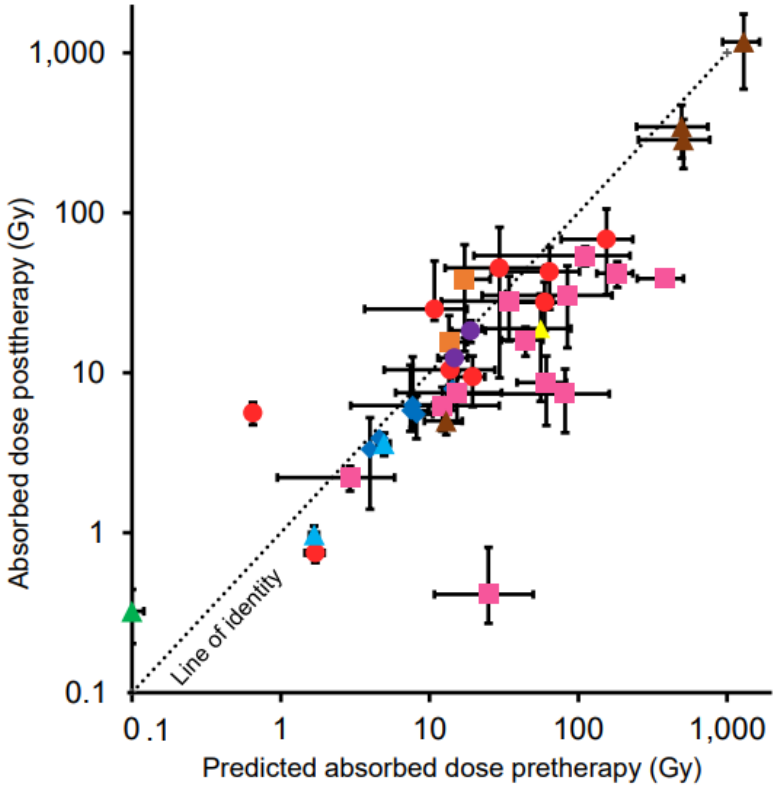

FIGURE 6: Comparison of absorbed doses for each lesion (colour coded by patient) as predicted from pre-therapy dosimetry and measured from post-therapy dosimetry.

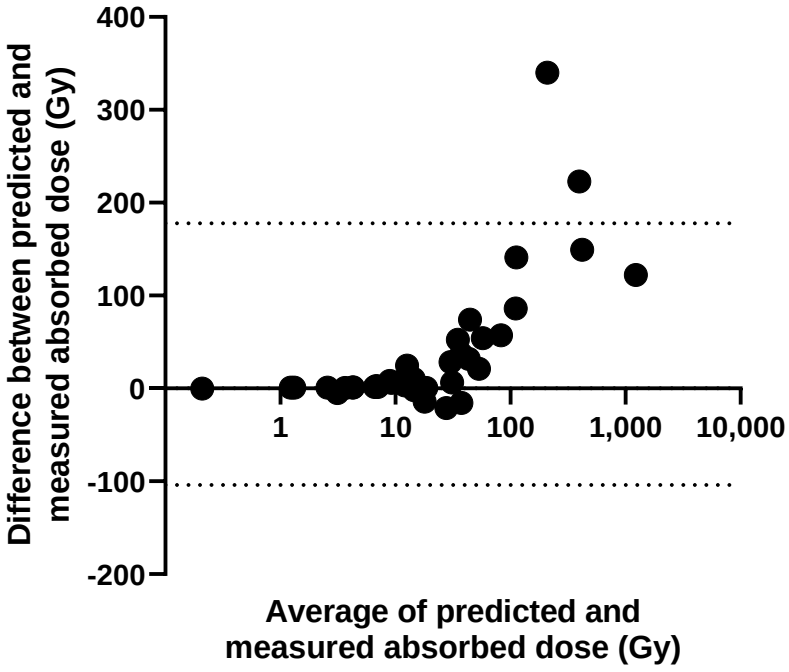

FIGURE 7: Bland–Altman plot for the comparison of absorbed doses predicted and measured for each lesion, showing the difference of predicted absorbed doses minus the actual delivered absorbed doses.

Graphical abstract